

Condensation Heat Transfer Enhancement on Surfaces with Interlaced Wettability

You-An Lee, Long-Sheng Kuo, Tsung-Wen Su, Chin-Chi Hsu, and Ping-Hei Chen*

Department of Mechanical Engineering, National Taiwan University, Taipei 10617, Taiwan

Abstract: This study investigated the effect of surfaces with interlaced wettability on steam-air mixture condensation. Experiments were conducted on various types of surface with different modified strip widths. In general, surfaces exhibiting high hydrophobic wettability yield a high condensation heat-transfer rate because dropwise condensation is easily formed. However, the experimental results of this study revealed that surfaces with interlaced wettability demonstrated superior condensation heat-transfer performance to those with homogeneous high hydrophobic wettability. Such an observation implies that the configuration of surface modification can enhance condensation heat transfer. In addition, the data indicated an optimal area ratio of modified surfaces to unmodified surfaces.

Keywords: Condensation heat transfer, interlaced wettability, surface modification.

1. INTRODUCTION

Water vapor condensation is a common physical phenomenon widely applied in various industries including water harvesting [1, 2], power generation [3], and thermal management in electronic device [4]. In the past decades, dropwise condensation has been reported to yield a heat transfer coefficient one order higher in magnitude compared with filmwise condensation [5, 6]. Numerous researchers have attempted to achieve dropwise condensation by employing various methods, including producing a superhydrophobic surface.

The surface can be made superhydrophobic by creating microstructure roughness on top by using lithography [7], layer-by-layer deposition [8], or sol-gel nanoparticle coating [9], and occasionally followed by attaching low surface energy material on top of the structure. However, maintaining dropwise condensation is difficult because of the durability of the hydrophobic coating and condensation occurring between the structures leading to wetting transition [10, 11]. To solve these problems, several attempts have been made to promote dropwise condensation by using nano-textured surfaces, leading to a breakthrough in this line of research [12-14]. The researchers modified the sample surfaces to have hierarchical structures with hydrophobic wettability, making the condensate shed the surface easily and rapidly, resulting in an efficient condensation process. For example, Chen [12] and Miljkovic [14] show the jumping phenomena of condensates by applying a compact hierarchical structure on condensing surfaces.

In addition to fabricating a hierarchical structured surface, other research has been conducted on surfaces patterned with different wettability to enhance heat-transfer performance and solve flooding problems that result in the degradation of the condensation rate under high-density conditions such as high heat flux, wall sub-cool, and super-saturation [13, 14]. Based on the condensation phenomena on the back of the Namib desert' beetles [15], these types of modification apply the advantage of both hydrophilic and hydrophobic surfaces. Condensation phenomena consist of several phases: nucleation, growth, coalescence, and removal [16]. Based on nucleation theory, the energy barrier for nucleation is lower on a hydrophilic surface, whereas the droplet removal frequency is higher on a hydrophobic surface [17, 18]. Thus, connecting and striking a balance for each phase of condensation is the key to enhancing condensation further [16].

Different implementations for such bi-philic surfaces are used, including matrix styles [19, 20], micro-interlaced strips [21, 22], and gradient wettability surfaces [23]. Studies have revealed a high potential for patterned surfaces to enhance heat-transfer efficiency. Instead of micro- or nano-scale patterns, Hsu [24] demonstrated that surfaces with macro-interlaced strip undergo substantial heat-transfer enhancement in boiling heat transfer, which renders the fabrication process easier compared with that for surfaces with micro- or nano- patterns.

This study examined the effect of a distinct pattern for enhanced steam-air mixture condensation on surfaces with macro-interlaced strips. We fabricated various types of interlaced surface with different modified strip widths that could be associated with the area ratio of modified regions on the surfaces, to

*Address correspondence to this author at the Department of Mechanical Engineering, National Taiwan University, Taipei 10617, Taiwan; Tel: +886 2 33662689; Fax: +886 2 23670781; E-mail: phchen@ntu.edu.tw

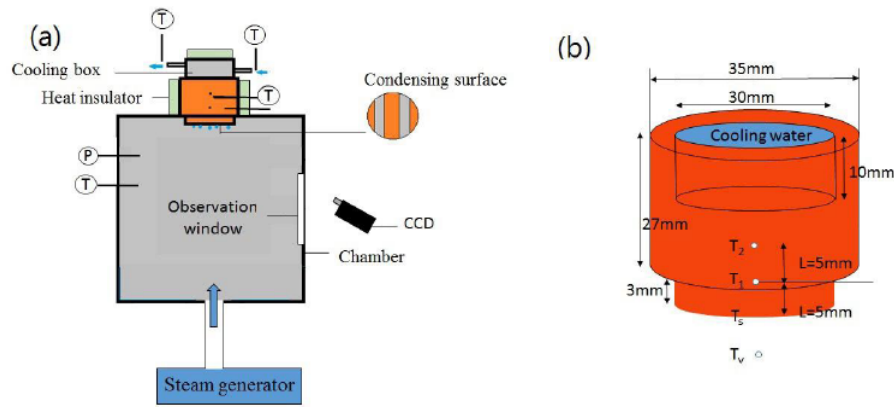


Figure 1: Experimental setup, (a) Thermal system and (b) Copper cylinder and temperature measurement location.

identify the balance of advantages between condensate nucleation and removal. These types of surface might have the potential to increase heat-transfer performance.

2. EXPERIMENTAL SYSTEM

Figure 1 illustrates the experimental setup. A copper cylinder 35 mm in diameter and 30 mm in height was used as a heat-transfer medium. One end of the cylinder functioned as the condensing surface horizontally facing downward. Thermocouples were inserted into the copper cylinder to measure the temperature gradient, followed by a calculation of surface temperature T_s by employing extrapolation as well as heat flux by using Fourier's law. The heat transfer coefficient was then obtained. T_1 and T_2 were determined individually according to the average of the two measured data at the same axial location. T_v is the average of the measured temperature of the saturated vapor. The uncertainties were ± 0.1 K for the thermocouples, and ± 0.5 mm for the location of temperature measurement.

Cooling water flowed through the other end of the cylinder in a groove, varying the wall sub-cool as an operating variable, which was nearly within 10 K. The

flow rate and inlet temperature of cooling water were controlled by the cooling circulator.

A pressure transducer was inserted to determine the concentration of the non-condensable gas, which was approximately 1.1% calculated using $W=(P-P_{atm})/P_{atm}$ in the configuration of the system. The charge-coupled device (CCD) camera from the side of the chamber records the condensation process during the experiments.

The uncertainties of the heat flux, wall sub-cool, and heat transfer coefficient within 2-10 K sub-cool were 5-10%, 2-10%, and 5-15% respectively.

3. SURFACE MODIFICATION

The sol-gel method was used to spin-coat nanoparticles on a copper surface. Table 1 lists the surface types and the corresponding parameters. The detailed procedure of preparing the solution is presented in Hsu's paper [25].

We heated the copper surfaces for 1.5 h at 120 °C after spinning. The second step was the preparation of hydrophobic materials by using fluoro-containing mixtures. Trichloro (1H, 1H, 2H, 2Hperfluorooctyl)

Table 1: List of the Surface Types and Corresponding Parameters

Surface Type	Modified Strip Width (a)	Plain Strip Width (b)	Modified Region CA	Plain Region CA
Plain	N/A	Whole surface	154.9°±3.1°	104.7°±3.8°
Super hydrophobic	Whole surface	N/A		
1.5/0.5	1.5mm	0.5mm		
2.5/0.5	2.5mm	0.5mm		
4.5/0.5	4.5mm	0.5mm		
5.5/0.5	5.5mm	0.5mm		

silane was mixed with methyl alcohol (1/100 in v/v). After spin coating the surface with the solution, the surfaces were heated at 90 °C for 40 min.

The interlaced wettability on the surface as produced by masking the specific strips before coating. The masks were removed afterward to obtain a relatively hydrophilic plain copper surface, which was fixed at a width of 0.5 mm in this study.

Contact angle measurements were conducted using the Sindatek Model 100SB. The contact angles (CAs) of the modified superhydrophobic and plain copper surfaces were $154.9^\circ \pm 3^\circ$ and approximately $104.7^\circ \pm 4^\circ$, respectively after being heated.

4. RESULTS AND DISCUSSION

Figure 2 presents the heat transfer coefficients at different sub-cool under different surface conditions. The modified surfaces with macro-interlaced strips and homogeneous superhydrophobicity clearly showed a superior heat transfer coefficient compared with the plain surface that exhibited filmwise condensation. In addition, the heat transfer coefficients for all types of surface seemed to decay and approach a certain constant value in our experiments. In pure steam condensation, the heat transfer coefficient increased with the rising sub-cool [5]. However, because of the accumulation and rising concentration of the non-condensable gas near the surface under high cooling intensity conditions, the heat transfer coefficient first decayed as the sub-cool began to increase and then yielded a constant value caused by the balance

between cooling intensity and the non-condensable gas effect.

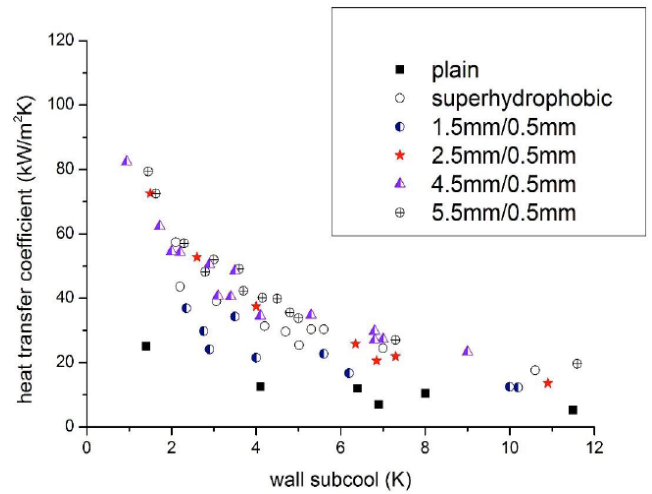


Figure 2: Variation of heat transfer coefficient with wall sub-cool for different types of surface.

4.1. Droplet Morphology on the Surfaces

Immediately after the entrance of saturated steam, nucleation occurred randomly on the homogeneous surfaces (plain and superhydrophobic). As the condensates grew and coalesced, a layer of liquid film formed on the plain surface, and the droplets on the superhydrophobic surfaces remained small and began to fall. The first and second rows of Figure 3 show a regular arrangement of nucleated condensates on the plain strips of the interlaced surfaces. However, because of the strip width magnitude and condensation process of relatively strong saturated vapor at

Stage (time)	Width --- superhydrophobic/plain (mm)				
	superhydrophobic	1.5/0.5	2.5/0.5	4.5/0.5	5.5/0.5
Initial (< 0.5mins)					
Growing (0.5~2mins)					
Steady (>5mins)					
Large Cooling intensity					

Figure 3: CCD images of the condensation processes on different types of Surfaces.

approximately 1 atm, few suspended droplets were observed to shed on a plain strip in a steady state.

Once the condensation process reaches the steady state, two processes exist for the condensates to leave the interlaced surface: one process is the direct removal of small droplets from the modified regions, and the other can be attributed to the connection between plain and modified regions, involving the movements of small droplets near the interfaces from modified strips to plain strips. Such movements of small droplets across the interface result from their coalescence with liquid film on the plain strips, forming suspended droplets that continually grow until the weight surpasses the surface tension force.

Few relatively large droplets were observed on the plain strips of the loosely inter-laced surfaces (4.5 mm, 5.5 mm), as shown in Figure 3. However, if two neighboring suspended droplets are exceedingly close to each other because of the narrow spacing and compact arrangement of strips, the suspended droplets on plain strips would coalesce to form super-large droplets crossing and hindering parts of modified regions, making the heat-transfer performance on the interlaced surfaces lower than that of the homogeneous superhydrophobic surfaces, as indicated by the 1.5/0.5 case shown in Figure 3.

The maximum diameters of the suspended droplets immediately before removal were affected by the presence of the modified strips. Suppose the droplet has a spherical shape immediately before falling and the length of the contact line is $b\pi$. By simple force balance, the size of the droplet before falling can be

determined using $r_{max} = \left(\frac{3\sigma b}{4\rho g}\right)^{\frac{1}{3}}$ where b is the plain pitch = 0.5 mm and $\sigma = 72.5$ mN/m. The widest diameter of the suspended droplets is then 2.81 mm.

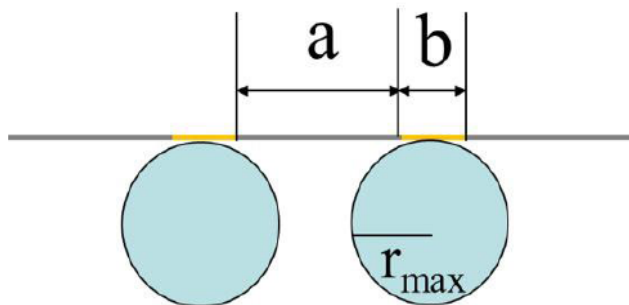


Figure 4: Illustration of the suspended droplets on plain strips.

According to Figure 4, we inferred the relation $\frac{a}{2} > \frac{D_{max}}{2} - \frac{b}{2}$ to prevent the coalescence of the nearby suspended droplets, where a is the modified width, b is the plain width, and $D_{max} = 2.81$ mm, which can be obtained from the aforementioned force balance. This value is consistent with the observation from CCD video, which is approximately 2.98 mm. Substituting all of the parameters into the aforementioned relation, the width of the modified strips should be wider than 2.31–2.48 mm, which matched well with our experimental results in that the 1.5-mm modified width led to the unwanted coalescence and formation of super-large droplets, whereas the 2.5-mm case did not. Although the large suspended droplets on the 2.5-mm surface did not coalesce, the compact arrangement of the droplets could serve as obstacles for steam to nucleate on the surface, reducing the heat transfer coefficient.

4.2. Area Ratio of Modified Regions

The condensates in the modified regions of the loosely interlaced surfaces were smaller than those on the homogeneous superhydrophobic surfaces, particularly under the high cooling intensity condition (the final row of Figure 3). Figure 5 presents the heat transfer coefficient as functions of the ratio of the modified areas on a surface. The ratio increased as the width of the modified strips increased and attained a value of 1 on the superhydrophobic surface. Generally, the overall heat transfer coefficient of an interlaced surface can be considered as the sum of contribution from each strip as

$$h = h_0 \left(1 - \frac{A_m}{A_{total}}\right) + h_m \frac{A_m}{A_{total}}$$

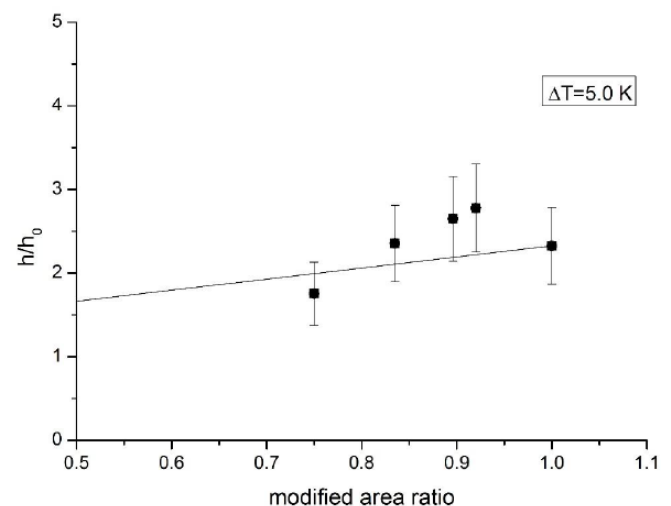


Figure 5: Heat transfer enhancement ratio as a function of the modified area ratio for the various types of modified surface when wall sub-cool = 5 K.

where h is the overall heat transfer coefficient, h_0 is the heat transfer coefficient of the plain copper surface, h_m is the heat transfer coefficient of the homogeneous superhydrophobic surface, A_m is the sum of the area of modified regions, and A_{total} is the area of the condensing surface. This relation is presented by line in Figure 5.

The measured data yielded higher values than the line for the interlaced surface except for the surface with 1.5-mm modified strips, the condensing surface of which was partially covered with large suspended droplets. Such an increase implied that the interlaced configuration additionally contributed to the heat transfer. The overall heat-transfer coefficient can be adjusted to

$$h = h_0 \left(1 - \frac{A_m}{A_{total}} \right) + h_m \frac{A_m}{A_{total}} + h_{interlace}$$

where $h_{interlace}$ is a variable depending on the modified area ratio and the wall sub-cool. The peak area ratio equal 0.9, implying that an optimal modified area ratio might exist to obtain the highest $h_{interlace}$. However, $h_{interlace}$ is a negative value if the width of the modified strips is excessively small, which diminishes the advantage of the interlaced surfaces because of surface blockage.

5. CONCLUSION

This study experimentally investigated the effects of surfaces with interlaced wettability on condensation heat transfer. The results show that the heat-transfer performance on interlace-patterned surfaces is higher than that on homogeneous superhydrophobic surfaces. Moreover, the growth of the droplet size as the wall sub-cool increased is less obvious on the interlace-patterned surfaces with large modified strips compared with those with homogeneous superhydrophobicity. This observation implies that the interlaced pattern may introduce an additional heat-transfer mechanism that could be attributed to enhancement and connection of different phases of the condensation process from nucleation to removal during condensation, compared with unpatterned surfaces. The optimal area ratio of the modified surfaces to the whole area is approximately 90%. Such an enhancement of heat transfer can be easily applied without complex fabrication processes, such as microelectromechanical systems, because the scale of the interlaced pattern is within the macro (millimeter) instead of micro or nano range.

ACKNOWLEDGEMENT

This work was supported by the Ministry of Science and Technology of Taiwan under project number MOST 102-2221-E-002-133-MY3, MOST 102-2221-E-002-088-MY3, and MOST 102-2218-E-002-022.

REFERENCES

- [1] Andrews HG, Eccles EA, Schofield WCE, Badyal JPS. Three-Dimensional Hierarchical Structures for Fog Harvesting. *Langmuir*. 2011; 5; 27(7):3798-802.
- [2] Lee A, Moon MW, Lim H, Kim WD, Kim HY. Water harvest via dewing. *Langmuir*. 2012 Jul 10;28(27):10183-91. <http://dx.doi.org/10.1021/la3013987>
- [3] Beer JM. High efficiency electric power generation: The environmental role. *Prog Energ Combust*. 2007 Apr;33(2):107-34. <http://dx.doi.org/10.1016/j.peecs.2006.08.002>
- [4] McGlen RJ, Jachuck R, Lin S. Integrated thermal management techniques for high power electronic devices. *Appl Therm Eng*. 2004 Jun; 24(8-9): 1143-56. <http://dx.doi.org/10.1016/j.applthermaleng.2003.12.029>
- [5] Rose JW. Dropwise condensation theory and experiment: a review. *P I Mech Eng a-J Pow*. 2002; 216(A2): 115-28.
- [6] Schmidt E, Schurig W, Sellschopp W. Condensation of water vapour in film- and drop form. *Z Ver Dtsch Ing*. 1930; 74: 544.
- [7] Oner D, McCarthy TJ. Ultrahydrophobic surfaces. Effects of topography length scales on wettability. *Langmuir*. 2000 Oct 3; 16(20): 7777-82. <http://dx.doi.org/10.1021/la000598o>
- [8] Bravo J, Zhai L, Wu ZZ, Cohen RE, Rubner MF. Transparent superhydrophobic films based on silica nanoparticles. *Langmuir*. 2007 Jun 19; 23(13): 7293-8. <http://dx.doi.org/10.1021/la070159g>
- [9] Rao AV, Lathe SS, Mahadik SA, Kappenstein C. Mechanically stable and corrosion resistant superhydrophobic sol-gel coatings on copper substrate. *Appl Surf Sci*. 2011 Apr 15; 257(13): 5772-6. <http://dx.doi.org/10.1016/j.apsusc.2011.01.099>
- [10] Narhe RD, Beysens DA. Growth dynamics of water drops on a square-pattern rough hydrophobic surface. *Langmuir*. 2007 Jun 5; 23(12): 6486-9. <http://dx.doi.org/10.1021/la062021y>
- [11] Cheng YT, Rodak DE. Is the lotus leaf superhydrophobic? *Appl Phys Lett*. 2005 Apr 4;86(14). <http://dx.doi.org/10.1063/1.1895487>
- [12] Boreyko JB, Chen CH. Self-Propelled Dropwise Condensate on Superhydrophobic Surfaces. *Phys Rev Lett*. 2009 Oct 30;103(18). <http://dx.doi.org/10.1103/PhysRevLett.103.184501>
- [13] Cheng JT, Vandadi A, Chen CL. Condensation heat transfer on two-tier superhydrophobic surfaces. *Appl Phys Lett*. 2012 Sep 24;101(13). <http://dx.doi.org/10.1063/1.4756800>
- [14] Miljkovic N, Enright R, Nam Y, Lopez K, Dou N, Sack J, *et al*. Jumping-Droplet-Enhanced Condensation on Scalable Superhydrophobic Nanostructured Surfaces. *Nano Lett*. 2013 Jan;13(1):179-87. <http://dx.doi.org/10.1021/nl303835d>
- [15] Parker AR, Lawrence CR. Water capture by a desert beetle. *Nature*. 2001 Nov 01;414(6859):33-4. <http://dx.doi.org/10.1038/35102108>
- [16] Beaini SS, Carey VP. Strategies for Developing Surfaces to Enhance Dropwise Condensation: Exploring Contact Angles,

- Droplet Sizes, and Patterning Surfaces. *J Enhanc Heat Transf.* 2013;20(1):33-42.
<http://dx.doi.org/10.1615/JEnhHeatTransf.2013006822>
- [17] Carey VP. Molecular dynamics simulations and liquid-vapor phase-change phenomena. *Microscale Therm Eng.* 2002 Jan-Mar;6(1):1-2.
<http://dx.doi.org/10.1080/108939502753428194>
- [18] Xiao R, Miljkovic N, Enright R, Wang EN. Immersion Condensation on Oil-Infused Heterogeneous Surfaces for Enhanced Heat Transfer. *Sci Rep-Uk.* 2013 Jun 13;3.
- [19] Yao CW, Alvarado JL, Marsh CP, Jones BG, Collins MK. Wetting behavior on hybrid surfaces with hydrophobic and hydrophilic properties. *Appl Surf Sci.* 2014 Jan 30;290:59-65.
<http://dx.doi.org/10.1016/j.apsusc.2013.10.188>
- [20] Chatterjee A, Derby MM, Peles Y, Jensen MK. Enhancement of condensation heat transfer with patterned surfaces. *Int J Heat Mass Tran.* 2014 Apr;71:675-81.
<http://dx.doi.org/10.1016/j.ijheatmasstransfer.2013.12.069>
- [21] Lo CW, Wang CC, Lu MC. Spatial Control of Heterogeneous Nucleation on the Superhydrophobic Nanowire Array. *Adv Funct Mater.* 2014 Mar;24(9):1211-7.
<http://dx.doi.org/10.1002/adfm.201301984>
- [22] Varanasi KK, Hsu M, Bhate N, Yang WS, Deng T. Spatial control in the heterogeneous nucleation of water. *Appl Phys Lett.* 2009 Aug 31;95(9).
<http://dx.doi.org/10.1063/1.3200951>
- [23] Macner AM, Daniel S, Steen PH. Condensation on Surface Energy Gradient Shifts Drop Size Distribution toward Small Drops. *Langmuir.* 2014 Feb 25;30(7):1788-98.
<http://dx.doi.org/10.1021/la404057g>
- [24] Hsu CC, Su TW, Chen PH. Pool boiling of nanoparticle-modified surface with interlaced wettability. *Nanoscale Res Lett.* 2012 May 18;7.
- [25] Hsu CC, Chen PH. Surface wettability effects on critical heat flux of boiling heat transfer using nanoparticle coatings. *Int J Heat Mass Tran.* 2012 Jun;55(13-14):3713-9.
<http://dx.doi.org/10.1016/j.ijheatmasstransfer.2012.03.003>

Received on 27-11-2014

Accepted on 08-12-2014

Published on 15-01-2015

DOI: <http://dx.doi.org/10.15377/2409-5826.2015.02.01.4>

© 2015 Lee et al.; Avanti Publishers.

This is an open access article licensed under the terms of the Creative Commons Attribution Non-Commercial License (<http://creativecommons.org/licenses/by-nc/3.0/>) which permits unrestricted, non-commercial use, distribution and reproduction in any medium, provided the work is properly cited.